Electronic Supplementary Material (ESI) for Journal of Materials Chemistry

Synthesis and photovoltaic properties of benzo[1,2-*b*:4,5-*b*′]dithiophene derivative-based polymers with deep HOMO levels

Heung Gyu Kim,[†a] Sae Byeok Jo,[†a] Chiyeoung Shim,[a] Jaewon Lee,[a] Jisoo Shin,[a] Eun Chul Cho,[b] Soo-Ghang Ihn,[c] Yeong Suk Choi,[c] Yungi Kim[c] and Kilwon Cho[*a]

[a] Department of Chemical Engineering, Pohang University of Science and Technology, Pohang, 790-784, Korea
[b] Department of Chemical Engineering, Hanyang University, Seong-dong gu, Seoul, 133-791, Korea
[c] Samsung Advanced Institute of Technology Samsung Electronics, Yongin, 446-712, Korea

Supporting Information

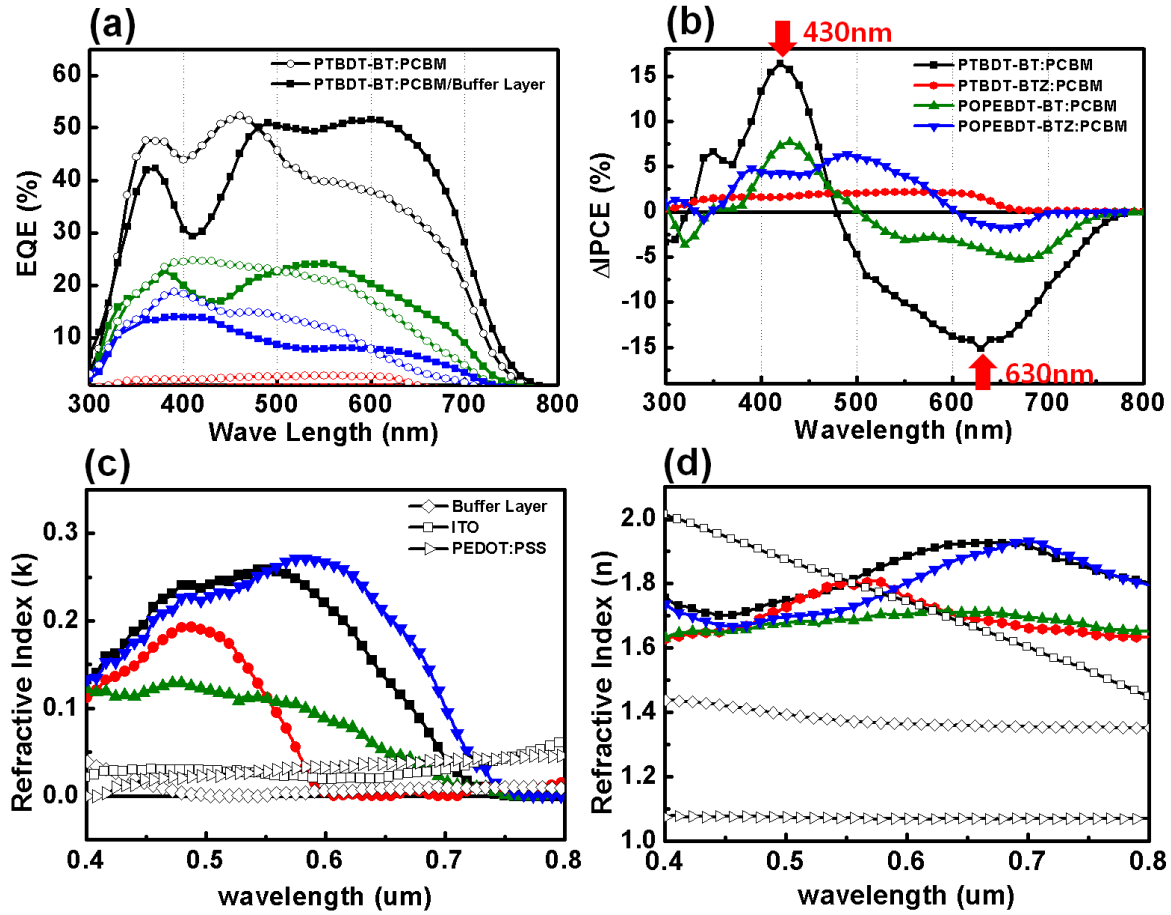

Fig. S1. (a) The EQE spectra of the devices comprising polymer:$PC_{71}BM$ blend with (open figures) and without (closed figures) cathode interlayer. (b) The difference between EQE spectra with and without cathode interlayers. The arrows indicate the position where the increase (430nm) and decrease (630nm) of EQE is observed. Measured (c) extinction coefficients and (d) refractive indices of each layers in the devices. These values were used for the optical simulations. The values for the Al electrode were obtained from the literature (A. D. Rakic, Appl. Opt. 1995, 34, 4755).

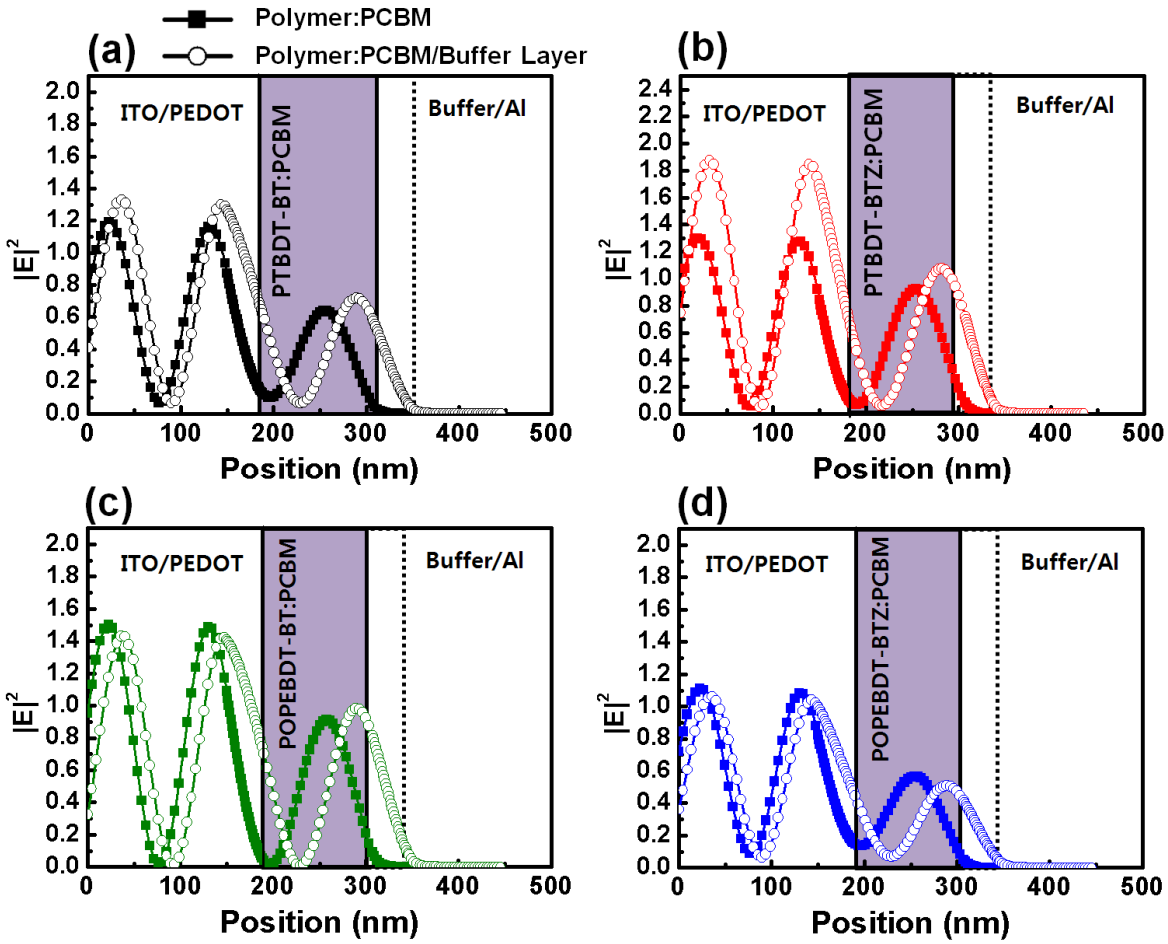

Fig. S2. Calculated spatial distribution of the electromagnetic fields inside devices comprising (a) PTBDT-BT (b) PTBDT-BTZ (c) POPEBDT-BT and (d) POPEBDT-BTZ with (open circle) and without (closed square) cathode interlayers at the wavelength of 430 nm. As shown in Fig. S1. (b), the optical electric fields clearly indicates increment in intensity with insertion layers.

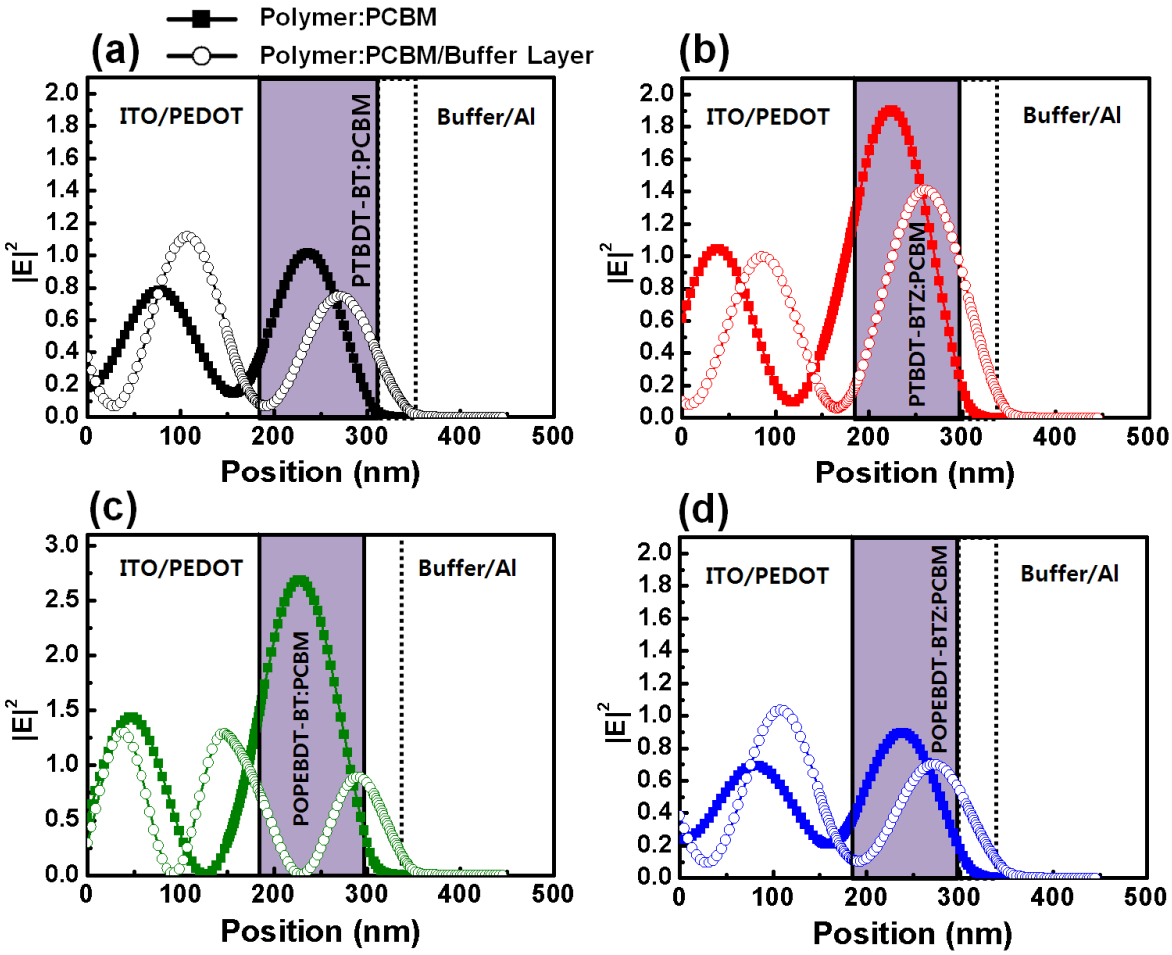

Fig. S3. Calculated spatial distribution of the electromagnetic fields inside devices comprising (a) PTBDT-BT (b) PTBDT-BTZ (c) POPEBDT-BT and (d) POPEBDT-BTZ with (open circle) and without (closed square) cathode interlayers at the wavelength of 630 nm. As shown in Fig.S1. (b), the optical electric fields clearly indicates decrement in intensity with insertion layers.

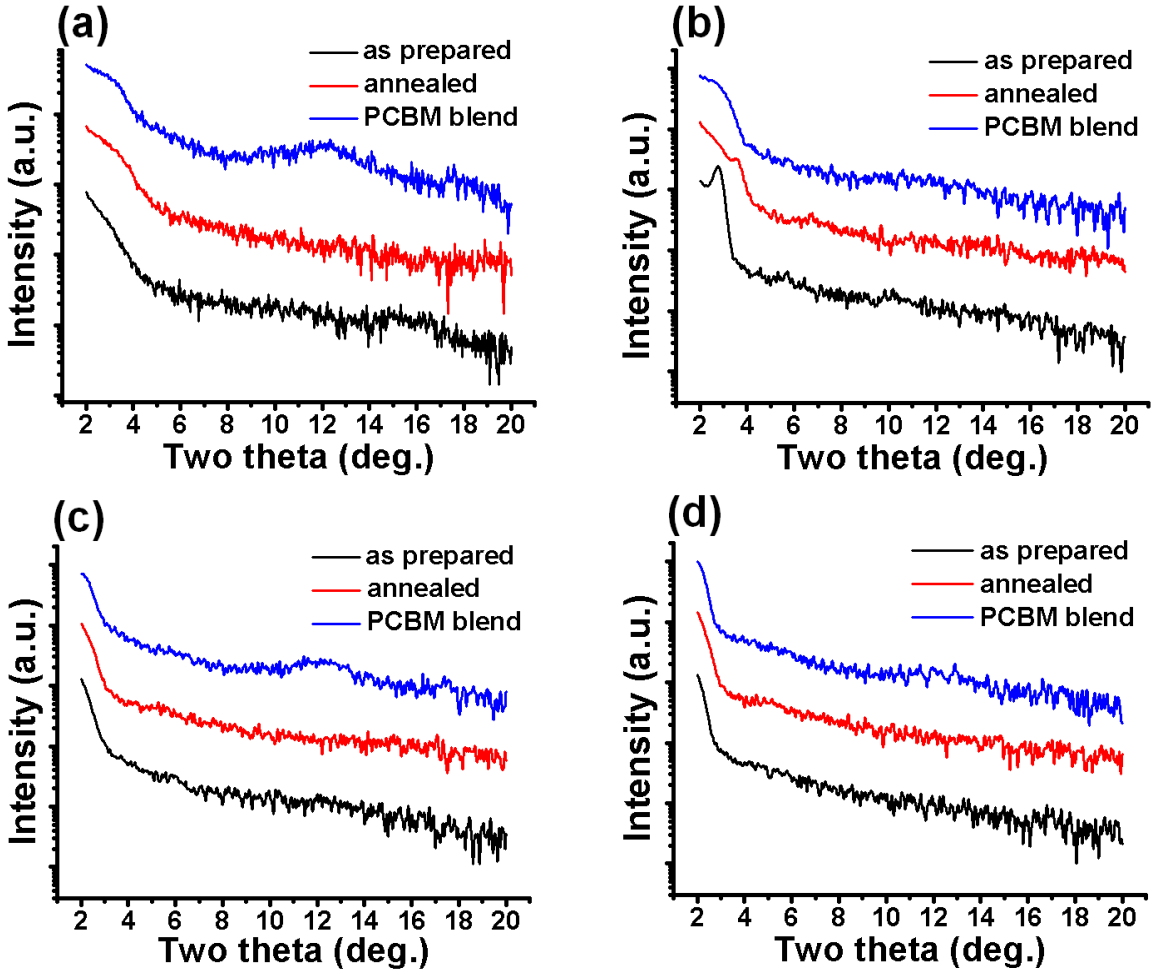

Fig. S4. X-ray scattering spectrum of the synthesized polymers (a) PTBDT-BT (b) PTBDT-BTZ (c) POPEBDT-BT and (d) POPEBDT-BTZ with different compositions and processing conditions. Aside from a slight appearance of a peak near 2.4 ° (2Theta) of PTBDT-BTZ, the polymers showed no significant crystallinity, especially within the blend with $PC_{71}BM$. A broad peak around 12 ° in all polymer blends corresponds to the PCBM hallow peak.

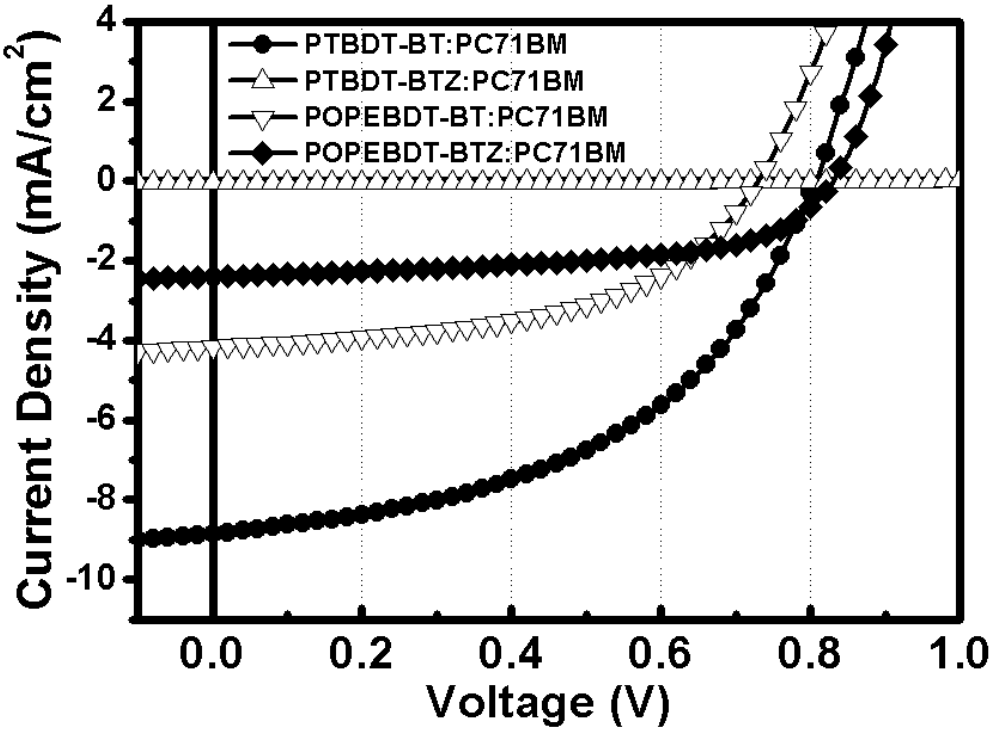

Fig. S5. *J-V* characteristics (AM 1.5G, 100 mW cm^{-2}) of the polymer:$PC_{71}BM$ blend devices without cathode insertion layers (PEGylated ZnO).

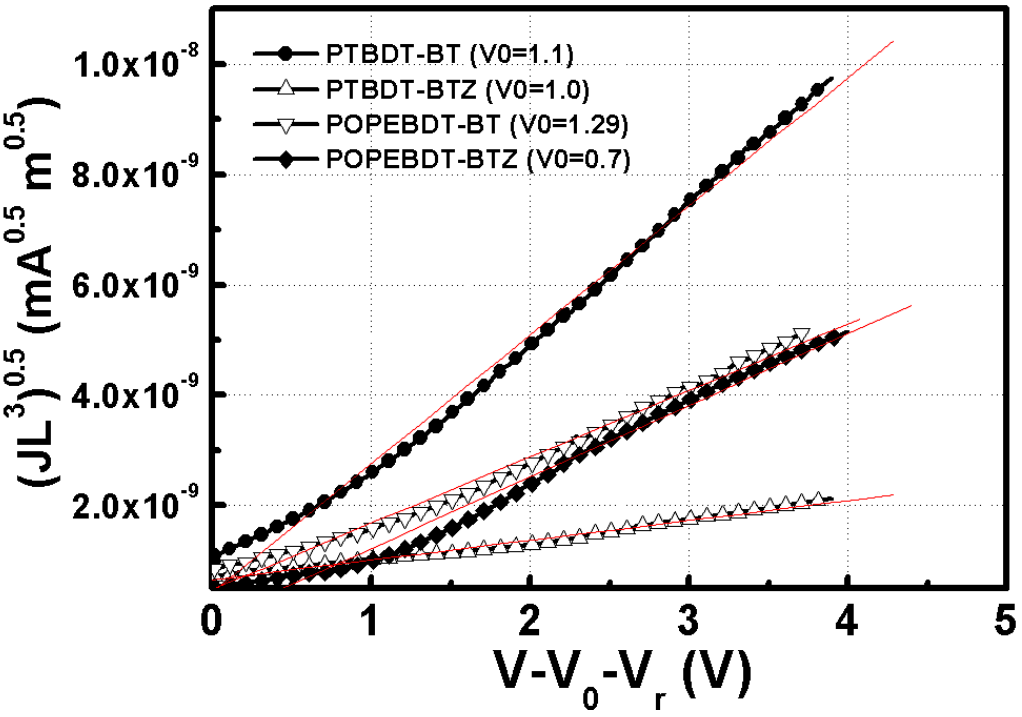

Fig. S6. The space charge limited current (SCLC) density measured with the structure of ITO/PEDOT:PSS/Active/Pd along with effective applied voltage. The effective voltage (V_{eff}) was calculated by subtracting built-in voltage (V_0) and voltage drop due to resistance (V_r) from the applied voltage (V). The V_0 was calculated by fitting the J-V curves in trap-free region using Mott-Gurney square law, (M. A. Lampert et al, Current injection in Solids; Academic Press; New York, 1970)

$$J = (9/8)\varepsilon\mu(V_{eff}^2/L^3)$$

where ε is the dielectric constant of the medium and the μ is the carrier mobility. The hole mobilities extracted from the currents in the square law region can be found in the main text.

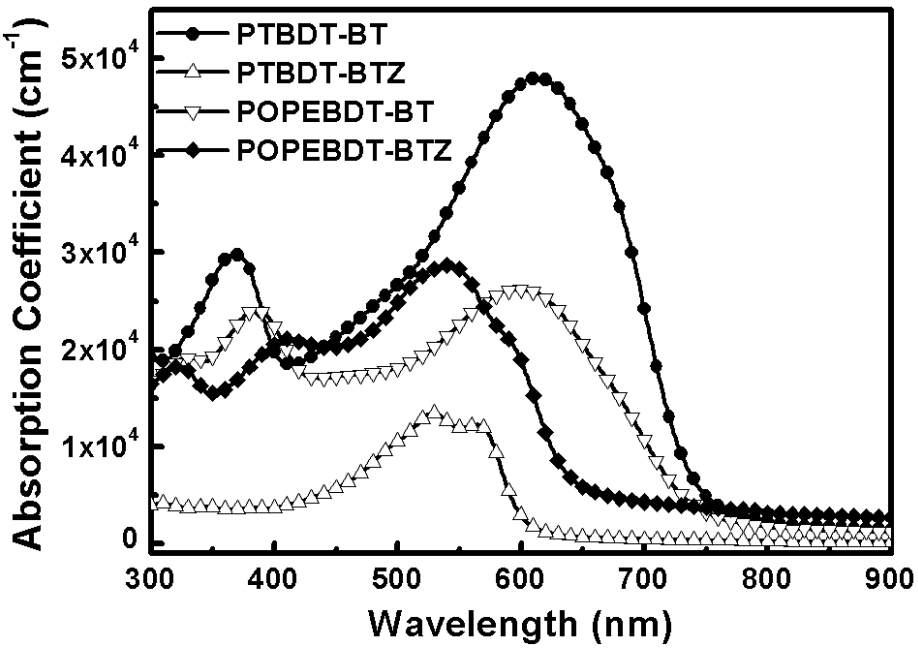

Fig. S7. The calculated absorption coefficients of the homo polymer films. The thickness of the polymer films were 40 nm for PTBDT-BT, 52 nm for PTBDT-BTZ, 57.5 nm for POPEBDT-BT, and 50 nm for POPEBDT-BTZ.